Variability and Uncertainty in Flux-Site Scale Net Ecosystem Exchange Simulations Based on Machine Learning and Remote Sensing: A Systematic Evaluation

Haiyang Shi[1,2,4,5], Geping Luo[1,2,3,5], Olaf Hellwich[6], Mingjuan Xie[1,2,4,5], Chen Zhang[1,2], Yu Zhang[1,2], Yuangang Wang[1,2], Xiuliang Yuan[1], Xiaofei Ma[1], Wenqiang Zhang[1,2,4,5], Alishir Kurban[1,2,3,5], Philippe De Maeyer[1,2,4,5] and Tim Van de Voorde[4,5]

[1] State Key Laboratory of Desert and Oasis Ecology, Xinjiang Institute of Ecology and Geography, Chinese Academy of Sciences, Urumqi, Xinjiang, 830011, China.
[2] University of Chinese Academy of Sciences, 19 (A) Yuquan Road, Beijing, 100049, China.
[3] Research Centre for Ecology and Environment of Central Asia, Chinese Academy of Sciences, Urumqi, China.
[4] Department of Geography, Ghent University, Ghent 9000, Belgium.
[5] Sino-Belgian Joint Laboratory of Geo-Information, Ghent, Belgium and Urumqi, China.
[6] Department of Computer Vision & Remote Sensing, Technische Universität Berlin, 10587 Berlin, Germany.

~~***Correspondence to*:** Geping Luo (luogp@ms.xjb.ac.cn) and Olaf Hellwich (olaf.hellwich@tu-berlin.de)~~

***Correspondence to*:** Geping Luo (luogp@ms.xjb.ac.cn) and Olaf Hellwich (olaf.hellwich@tu-berlin.de)

Submitted to *Biogeosciences*

Abstract. Net ecosystem exchange (NEE) is an important indicator of carbon cycling in terrestrial ecosystems. Many previous studies have combined flux observations, meteorological, biophysical, and ancillary predictors using machine learning to simulate the site-scale NEE. However, systematic evaluation of the performance of such models is limited. Therefore, we performed a meta-analysis of these NEE simulations. A total of 40 such studies and 178 model records were included. The impacts of various features throughout the modeling process on the accuracy of the model were evaluated. Random Forests and Support Vector Machines performed better than other algorithms. Models with larger time scales have lower average R-squared, especially when the time scale exceeds the monthly scale. Half-hourly models (average R-squared = 0.73) were significantly more accurate than daily models (average R-squared = 0.5). There are significant differences in the predictors used and their impacts on model accuracy for different plant functional types (PFTs). Studies at continental and global scales (average R-squared = 0.37) with multiple PFTs, more sites, and a large span of years correspond to lower R-squared than studies at local (average R-squared = 0.69) and regional scales (average R-squared = 0.7). Also, the site-scale NEE predictions need more focus on the internal heterogeneity of the NEE dataset and the matching of the training set and validation set.

1 Introduction

Net ecosystem exchange (NEE) of CO_2 is an important indicator of carbon cycling in terrestrial ecosystems (Fu et al., 2019), and accurate estimation of NEE is important for the development of global carbon neutral policies. Although process-based models have been used for NEE simulations (Mitchell et al., 2009), their accuracy and spatial resolutions of the model outputs are limited probably due to the lack of understanding and quantification of complex processes. Many researchers have tried to use a data-driven approach as an alternative (Fu et al., 2014; Tian et al., 2017; Tramontana et al., 2016; Jung et al., 2011). On the one hand, it was made possible by the increase in the growth of global carbon flux observations and the large amount of flux observation data being accumulated. Since the 1990s, the use of the eddy covariance technique to monitor NEE has been rapidly promoted (Baldocchi, 2003). Several regional and global flux measurement networks have been established for the big data management of the flux sites, including CarboEuro-flux (Europe), AmeriFlux (North America), OzFlux (Australia), ChinaFlux (China), FLUXNET (global), etc. On the other hand, machine learning approaches are increasingly used to extract patterns and insights from the ever-increasing stream of geospatial data (Reichstein et al., 2019). The rapid development of various algorithms and high public availability of model tools in the field of machine learning have made these techniques easily available to more researchers in the field of geography and ecology (Reichstein et al., 2019). Since the above two major advances (i.e., increasing availability of flux data and machine learning techniques) in the last two decades, various machine learning algorithms have been used to simulate NEE at the flux station scale with various predictor variables (e.g., meteorological variables, biophysical variables) incorporated for spatial and temporal mapping of NEE or understanding the driving mechanisms of NEE.

To date, studies on using machine learning to predict NEE have a high diversity in terms of modeling approaches. To obtain a comprehensive understanding of machine learning-based NEE prediction, a synthesis evaluation of these machine learning models is necessary. Since the beginning of this century, when machine

learning approaches were still rarely used in geography and ecology research, neural networks were already used to perform simulations and mapping of NEE in European forests (Papale and Valentini, 2003). Subsequently, considerable efforts have been made by researchers to improve such predictive models. Many studies have demonstrated the effectiveness of their proposed improvements (i.e., using predictors with a higher spatial resolution (Reitz et al., 2021) and using data from the local flux site network (Cho et al., 2021)) by comparing with previous studies. However, the improvements achieved in these studies may be limited to smaller areas and specific conditions and may not be generalizable (Cleverly et al., 2020; Reed et al., 2021; Cho et al., 2021). We are more interested in guidelines with universal applicability that improve the model accuracy, such as the selection of appropriate predictors and algorithms under different conditions. Therefore, we should synthesize the results of models applied to different conditions and regions to obtain general insights.

Many factors may affect the performance of these NEE prediction models, such as the predictor variables, the spatial and temporal span of the observed flux data, the plant functional type (PFT) of the flux sites, the model validation method, the machine learning algorithm used, as described below:

a) ~~Predictors: Various biophysical variables (Zeng et al., 2020; Cui et al., 2021; Huemmrich et al., 2019)~~Predictors: Various biophysical variables (Zeng et al., 2020; Cui et al., 2021; Huemmrich et al., 2019) and other meteorological and environmental factors have been used in the simulation of NEE. The most commonly used predictor variables include precipitation (Prec), air temperature (Ta), wind speed (Ws), net/sun radiation (Rn/Rs), soil temperature (Ts), soil texture, soil moisture (SM) (Zhou et al., 2020), vapor-pressure deficit (VPD) (Moffat et al., 2010; Park et al., 2018), the fraction of absorbed photosynthetically active radiation (FAPAR) (Park et al., 2018; Tian et al., 2017), vegetation index (e.g., NDVI, EVI), LAI, and evapotranspiration (ET) (Berryman et al., 2018). The predictor variables used vary with the natural conditions and vegetation functional types of the study area. In contrast, in models that include multiple PFTs, some variables that play a significant role in the prediction of each of the multiple PFTs may have higher importance. For example, growing degree days (GDD) may be a more effective variable for NEE of tundra in the northern hemisphere high latitudes (Virkkala et al., 2021), while measured groundwater levels may be important for wetlands (Zhang et al., 2021). Some of these predictor variables are measured at flux stations (e.g., meteorological factors such as precipitation and temperature), while others are extracted from reanalyzed meteorological datasets and satellite remote sensing image data (e.g., vegetation indices). The spatial and temporal resolution of predictors can lead to differences in their relevance to NEE observations. Most measured in situ meteorological factors have a good spatio-temporal match to the observed NEE (site scale, half-hourly scale). However, the proportion of NEE explained by remotely sensed biophysical covariates may depend on their spatial and ~~temporal~~time scales. For example, the MODIS-based 8-daily NDVI data may better capture temporal variation in the relationship between NEE and vegetation growth than the Landsat-based 16-daily NDVI data. In contrast, the interpretation of NEE by variables such as soil texture and soil organic content (SOC), which do not have temporal dynamic information, may be limited to the interpretation of spatial variability, although they are considered to be important drivers of NEE. Therefore, the importance of variables obtained from NEE simulations based on a data-driven approach may differ from that in process-based models as well as in the actual driving mechanisms. This may be related to the spatial and temporal resolution of the predictors used and the

quality of the data. It is necessary to consider the spatio-temporal resolution of the data for the actual biophysical variables used in the different studies in the systematic evaluation of data-driven NEE simulations.

b) The spatio-temporal heterogeneity of data sets, and validation method: The spatio-temporal heterogeneity of the dataset may affect model accuracy. Typically, training data with larger regions, multiple sites, multiple PFTs, and longer spans of years may have a higher degree of imbalance ~~(Kaur et al., 2019; Van Hulse et al., 2007; Virkkala et al., 2021; Zeng et al., 2020)~~(Kaur et al., 2019; Van Hulse et al., 2007; Virkkala et al., 2021; Zeng et al., 2020). Modeling with unbalanced data (where the difference between the distribution of the training and validation sets is significant even if selected at random) may result in lower model accuracy. To date, the most commonly used methods for validating such models include spatial (Virkkala et al., 2021), temporal (Reed et al., 2021), and random (Cui et al., 2021) cross-validation. The imbalance of data between the training and validation sets may affect the accuracy of the models when using these validation methods. Spatial validation is used to assess the ability of the model to adapt to different regions or flux sites of different PFTs, and a common method is 'leave one site out' cross-validation ~~(Virkkala et al., 2021; Zeng et al., 2020)~~(Virkkala et al., 2021; Zeng et al., 2020). If the data from the site left out is not covered (or partially covered) by the distribution of the training dataset, the model's prediction performance at that site may be poor due to the absence of a similar type in the training set. Temporal validation typically uses some years of data as training and the remaining years as validation to assess the model's fitness for interannual variability. For a year that is left out (e.g. a special extreme drought year which does not occur in the training set), the accuracy of the model may be limited if there are no similar years (extreme drought years) in the training dataset. K-fold cross-validation is commonly used in random cross-validation to assess the fitness of the model to the spatio-temporal variability. In this case, different values of K may also have a significant impact on the model accuracy. For example, for an unbalanced dataset, the average model accuracy obtained from a 10-fold (K = 10) validation approach is likely to be higher than that of a 3-fold (K = 3) validation approach (Marcot and Hanea, 2021).

c) Machine learning algorithms used: Simulating NEE using different machine learning algorithms may influence the model accuracy, which may be induced by the characteristics of these algorithms themselves and the specific data distribution of the NEE training set. For example, Neural Networks can be used effectively to deal with nonlinearities, while as an ensemble learning method, Random Forests can avoid overfitting due to the introduction of randomness. Therefore, a comprehensive evaluation of this is necessary.

In this study, to evaluate the impacts of predictors use, algorithms, spatial/~~temporal~~time scale, and validation methods on model accuracy, we performed a meta-analysis of papers with prediction models that combine NEE observations from flux towers, various predictors, and machine learning for the data-driven NEE simulations. In addition, we also analyzed the causality of multiple features in NEE simulations and the joint effects of multiple features on model accuracy using the Bayesian Network (BN) (a multivariate statistical analysis approach (Pearl, 1985)). The findings of this study can provide some general guidance for future NEE simulations.

2 Methodology

2.1 Criteria for including articles

In the Scopus database, a literature query was applied to titles, abstracts, and keywords (Table 1) according to Preferred Reporting Items for Systematic Reviews and Meta-Analyses (PRISMA) (Moher et al., 2009) (Fig. 1):

a) Articles were filtered for those that modeled NEE. Articles that modeled other carbon fluxes such as methane flux were not included.

b) Articles that used only univariate regression rather than multiple regression were screened out.

c) Articles reported the determination coefficient (R-squared) of the validation step ~~(Shi et al., 2021; Tramontana et al., 2016; Zeng et al., 2020)~~(Shi et al., 2021; Tramontana et al., 2016; Zeng et al., 2020) as the measure of model performance. Although RMSE is also often used for model accuracy assessment, its dependence on the magnitude of water flux values makes it difficult to use for fair comparisons between studies.

d) Articles were published in journals with language limited to English.

e) Articles were filtered for those that were published in the specific journals (Table S1) for research quality control because the data, model implements, and peer review in these journals are often more reliable.

Table 1. Article search query design: '[A1 OR A2 OR A3...] AND [B1 OR B2...] AND [C1 OR C2...]'

ID	A	B	C
1	Carbon flux	"Eddy covariance"	"machine learning"
2	CO_2 flux	"Flux tower"	regress*
3	"net ecosystem exchange"		"Support Vector"
4	net ecosystem produc		"Neural Network"
5	gross primary produc		"Random Forest"
6	Carbon exchange		

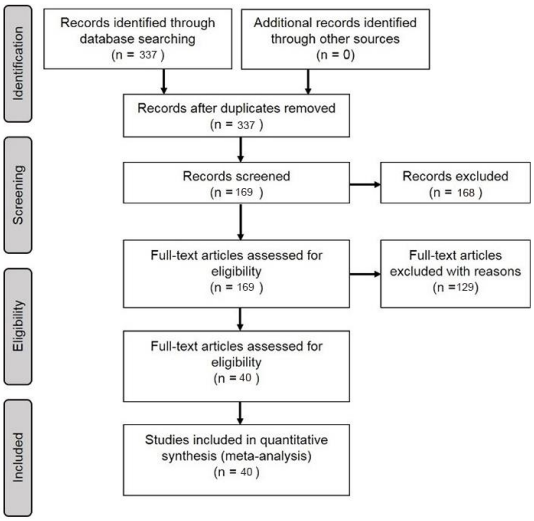

Figure 1. PRISMA-based paper filtering flowchart.

2.2 Features of prediction models

Typically, the flow of the NEE prediction modeling framework (Fig. 2) based on flux observations and machine learning is as follows: first, half-hourly scale NEE flux observations are aggregated into various time scale NEE data, and gap-filling techniques (Moffat et al., 2007) are often used in this step to obtain complete NEE series when data are missing. Various predictors including meteorological variables, remote sensing-based biophysical variables, etc. are extracted to match site-scale NEE series to generate a training dataset containing the target variable NEE and various covariates. Subsequently, various algorithms are used for the NEE prediction model construction and validated in different ways (e.g., leave-one-site-out validation (Zeng et al., 2020)). Finally, in some studies, prediction models were applied on gridded covariate data to map the regional or global-scale NEE spatial and temporal variations (Zeng et al., 2020; Papale and Valentini, 2003; Jung et al., 2020). The information of R-squared (at the validation phase) and the associated model features reported in the article are considered as one data record for the formal meta-analysis (i.e., each R-squared record corresponding to a prediction model). From the included papers, R-squared records and various features (Table 2) involved in the NEE modeling framework (Fig. 2) were extracted (including the used algorithms, modeling/validation methods, remote sensing data, meteorological data, biophysical data, and ancillary data). In some studies, multiple algorithms were applied to the same dataset, or models with different features were developed (Virkkala et al., 2021; Zhang et al., 2021; Cleverly et al., 2020; Tramontana et al., 2016). In these cases, multiple data records will be documented.

设置了格式：字体：Times New Roman

In the practical information extracting step, we categorized such features in a comparable manner. First, we categorized the various algorithms used in these papers, although the same algorithm may also have a variant

form or an optimized parameter scheme. They are categorized into the following families of algorithms: Random Forests (RF), Multiple Linear Regressions (MLR), Artificial Neural Networks (ANN), Support Vector Machines (SVM), Partial Least Squares Regression (PLSR), Generalized additive model (GAM), Boosted Regression Tree (BRT), Bayesian Additive Regression Trees (BART), Cubist, model tree ensembles (MTE). Second, we classified the spatial scales of these studies. Models with study areas (spatial extent covered by flux stations) smaller than 100x100 km were classified as 'local' scale models, those with study area sizes exceeding continental scale were classified as 'global' scale, and those with study area sizes in between were classified as 'regional' scale. Third, for various predictors, we only recorded whether the predictors were used or not without distinguishing the detailed data sources and categories (e.g., grid meteorological data from various reanalysis datasets and in-situ meteorological observations from flux stations), measurement methods (e.g., soil moisture measured/estimated by remote sensing or in situ sensors), etc. Fourth, we documented PFTs for the prediction models from the description of study areas or sites in these papers. They are classified into the following types: forest, grassland, cropland, wetland, savannah, tundra, and multi-PFTs (models containing a mixture of multiple PFTs). Models not belonging to the above PFTs were not given a PFT field and were not included in the subsequent analysis of the PFT differences. Other features (Table 2) are extracted directly from the corresponding descriptions in the papers in an explicit manner.

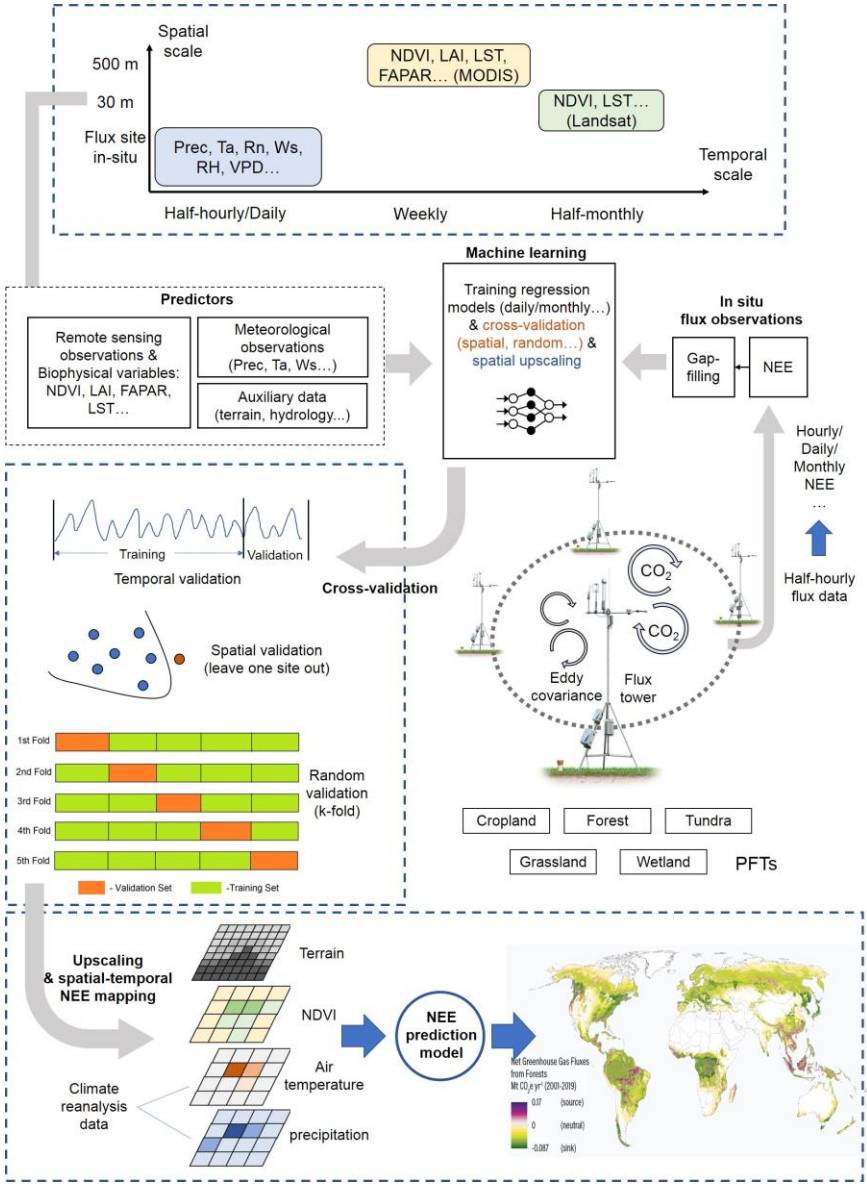

Figure 2. Features of the machine learning-based NEE prediction process. The flux tower photo is from https://www.licor.com/env/support/Eddy-Covariance/videos/ec-method-02.html (last accessed: 23rd March 2022). The map in the lower part is from Harris et al., 2021. Prec, Ta, Rn, Ws, RH, and VPD represent precipitation, air temperature, net surface radiation, wind speed, relative humidity, and vapour-pressure deficit respectively. FAPAR is the fraction of absorbed photosynthetically active radiation. LST is the land surface temperature. LAI is the leaf area index.

Subsequently, the model accuracies corresponding to different levels of various features are compared in a cross-study fashion. In the evaluation of algorithms and time scales, we also implement comparisons within individual studies. For example, in the evaluation of the effects of the algorithms, we compare the accuracy of models using the same training data and keeping other features as constants in individual studies. In this intra-study comparison step, only algorithms with relatively large sample sizes in the cross-study comparisons were selected.

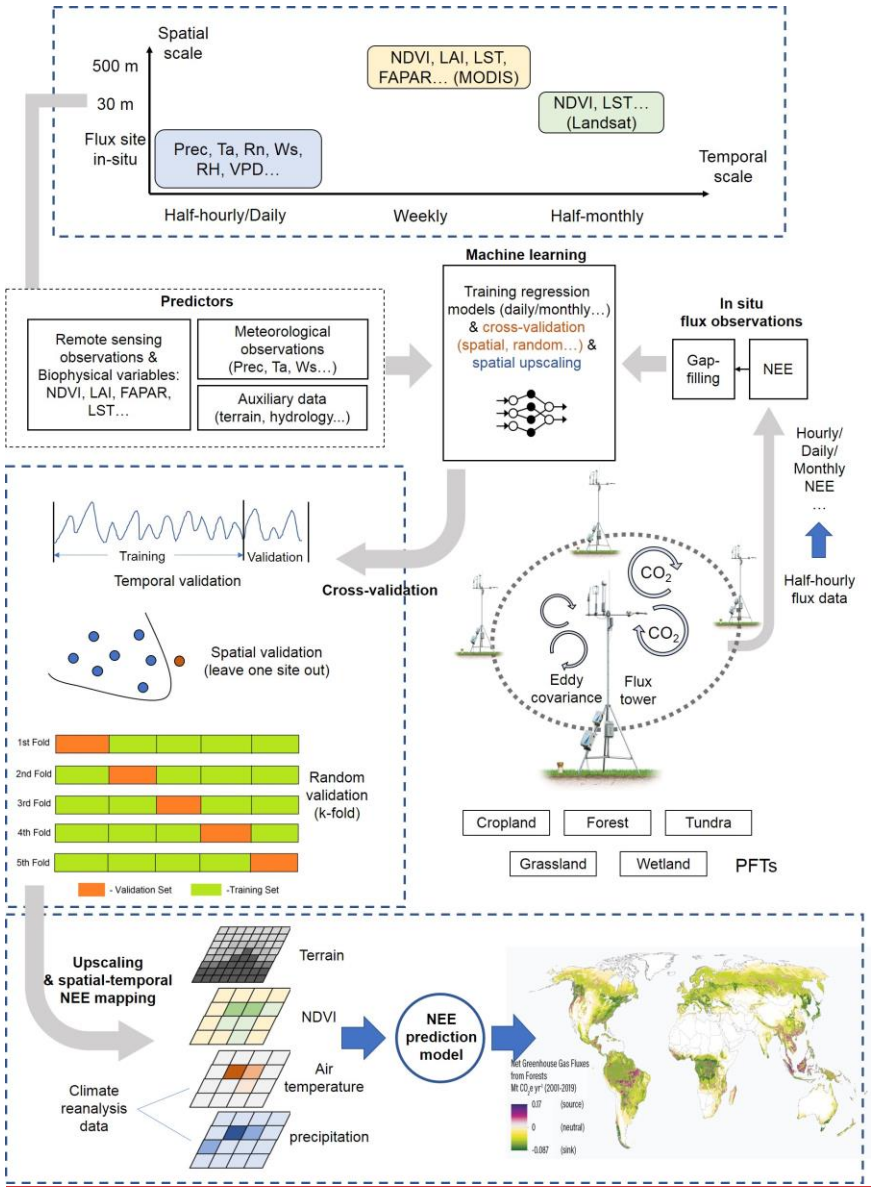

Figure 2. Features of the machine learning-based NEE prediction process. The flux tower photo is from https://www.licor.com/env/support/Eddy-Covariance/videos/ec-method-02.html (last accessed: 23rd March 2022). The map in the lower part is from Harris et al., 2021. Prec, Ta, Rn, Ws, RH, and VPD represent precipitation, air temperature, net surface radiation, wind speed, relative humidity, and vapour-pressure deficit respectively. FAPAR is the fraction of absorbed photosynthetically active radiation. LST is the land surface temperature. LAI is the leaf area index.

215

216 Table 2. Description of information extracted from the included papers.

Field/Feature	Definition	Categories adopted
Id paper	Identification number of the paper (internal)	
Paper	Paper metadata	
Author/s	Name/s of author/s	
Title	Title of the paper	
Year	Year of publication	
Publication title	Name of the journal where the paper was published	
Plant functional type (PFT)	PFTs for the flux sites used	1-forest, 2-grassland, 3-cropland, 4-wetland, 5-savannah, 6-tundra and multi-PFTs
Location	More precise location (with the latitude and longitude of the center of the studied sites). Global (mainly based on FluxNet (Tramontana et al., 2016)) and continental-scale studies are not shown on the map due to the difficulty of identifying specific locations.	latitude, longitude
Algorithms	Algorithm families used in the multivariate regression	Random Forests (RF), Multiple Linear Regressions (MLR), Artificial Neural Networks (ANN), Support Vector Machines (SVM), Partial Least Squares Regression (PLSR), Generalized additive model (GAM), Boosted Regression Tree (BRT), Bayesian Additive Regression Trees (BART), Cubist, model tree ensembles (MTE).
Sites number	Number of the flux sites used	
Study area/Spatial scale	Area representatively covered by the flux sites	local (less than 100×100 km), regional, global (continent-scale and global scale)
~~Temporal~~Time scale	The ~~temporal~~time scale of the model	half-hourly, hourly, daily, weekly, 8-daily, monthly, seasonally, yearly
Study period	The period of the data used in the model	year, growing season, daytime, spring, summer, autumn, winter
Year span	The span of years of the flux data used	
Site year	Describe the volume of total flux data with the number of sites and years aggregated.	
Cross-validation	Describe the chosen method of cross-validation.	Spatial (e.g., 'leave one site out'), temporal (e.g., 'leave one year out'), random (e.g., 'k-fold')

Training/validation	Describe the ratio of the data in training and validation sets.	
Satellite images	Describe the source of satellite images used to derive NDVI, EVI, LAI, LST, etc.	Landsat, MODIS, Hyperion (EO-1), AVHRR, IKONOS
Biophysical predictors	LAI, NDVI/EVI, evapotranspiration (ET) (i.e., the latent heat observed by the flux station), enhanced vegetation index (EVI), the fraction of absorbed photosynthetically active radiation/photosynthetically active radiation (FAPAR/PAR), leaf area index (LAI), etc.	Used (recorded as '1') or not used (recorded as '0')
Meteorological variables	precipitation (Prec), net radiation/solar radiation (Rn/Rs), air temperature (Ta), vapour-pressure deficit (VPD), relative humidity (RH) , etc.	Used (recorded as '1') or not used (recorded as '0')
Ancillary data	Describe the source of ancillary variables including terrain variables derived from DEM, soil texture, or hydrology-related data: soil organic content (SOC), soil texture, terrain, soil moisture/land surface water index (SM_LSWI), etc.	Used (recorded as '1') or not used (recorded as '0')
Top three variables in the ranking of importance of predictors	Describe the interpretation of the importance of variables in machine learning models.	
Accuracy measure	Accuracy measure used to assess the performance of the estimation/prediction	R-squared (in the validation phase)

2.3 Bayesian Network for analyzing joint effects

Based on the Bayesian network (BN), the joint impacts of multiple model features on the R-squared are analyzed. A BN can be represented by nodes (X_1,., X_n) and the joint distribution (Pearl, 1985):

$$P(X) = P(X_1, X_2, \dots, X_n) = \prod_{i=1}^{n} P\left(X_i \middle| pa(X_i)\right) \quad (1)$$

where $pa(X_i)$ is the probability of the parent node X_i. Expectation-maximization (EM) approach (Moon, 1996) is used to incorporate the collected model records and compile the BN.

Sensitivity analysis is used for the evaluation of node influence based on mutual information (MI) which is calculated as the entropy reduction of the child node resulting from changes at the parent node (Shi et al., 2020):

$$MI = H(Q)-H(Q|F)=\sum_q \sum_f P(q, f) \log_2 \left(\frac{P(q,f)}{P(q)P(f)}\right) \quad (2)$$

where H represents the entropy, Q represents the target node, F represents the set of other nodes and q and f represent the status of Q and F.

3 Results

3.1 Articles included in the meta-analysis

We included 40 articles (Table S2) and extracted 178 model records for the formal meta-analysis (Fig. 1). Most studies were implemented in Europe, North America, Oceania, and China (Fig. 3). The number of such papers is increasing recently (Fig. 4) and it shows the machine learning approach for NEE prediction has been of interest to more researchers. The main journals in which these articles have been published (Fig. 4) include Remote Sensing of Environment, Global Change Biology, Agricultural and Forest Meteorology, Biogeosciences, and Journal of Geophysical Research: Biogeosciences, etc.

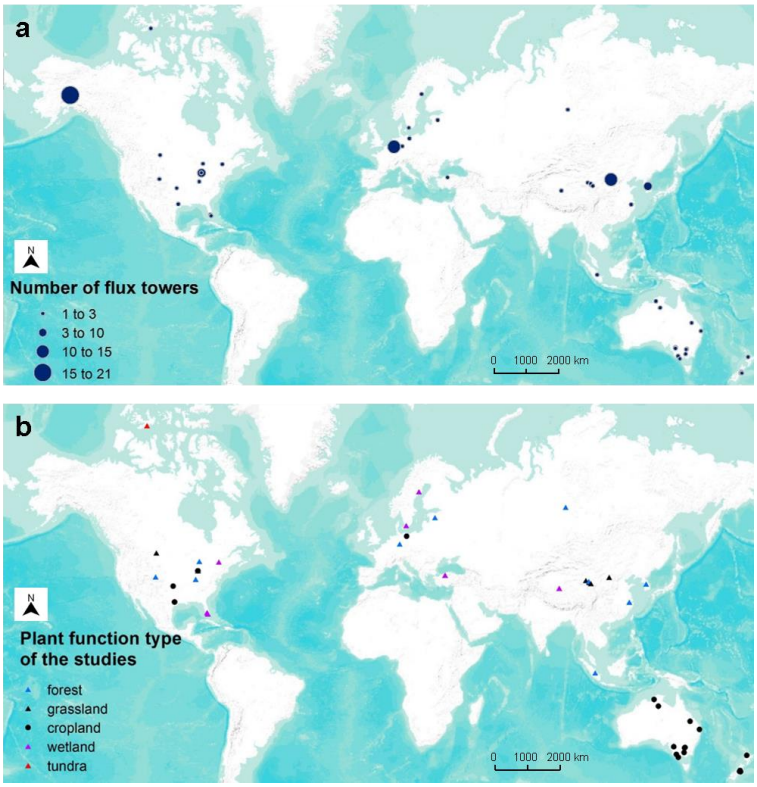

Figure 3. Location of studies (a) included with the number of flux sites included and (b) their PFTs in the meta-analysis (total of 40 studies and 178 model records). Global (mainly based on FluxNet (Tramontana et al.,

2016)) and continental-scale studies are not shown on the map due to the difficulty of identifying specific locations.

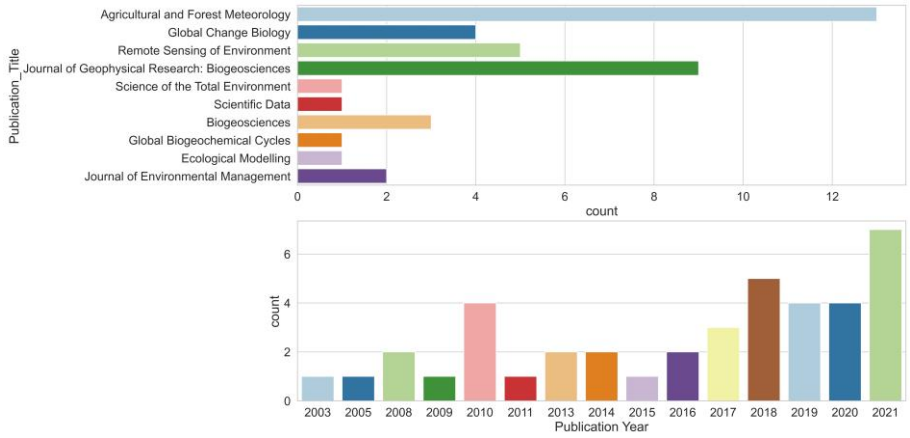

Figure 4. The number of studies published across journals and the total number of publications per year.

3.2 The formal Meta-analysis

We assessed the impact of the features (e.g., algorithms, study area, PFTs, amount of data, validation methods, predictor variables, etc.) used in the different models based on differences in R-squared.

3.2.1 Algorithms

Among the more frequently used algorithms, ANN and SVM performed better (Fig. 5a) on average across studies (lightly better than RF). On the other hand, since cross-study comparisons of algorithm accuracy include differences in data used in model construction, we performed a pairwise comparison (Fig. 5b) of these four algorithms (i.e., ANN, SVM, RF, and MLR). In these studies, multiple models are developed for consistent training data with the interference of training data differences removed. It shows that RF and SVM perform best in the inter-study comparison (Fig. 5b). Whereas ANN performed slightly worse than RF and SVM, all three of them were stronger than MLR. Overall, the performance of RF and SVM may be good and similar in the NEE simulations.

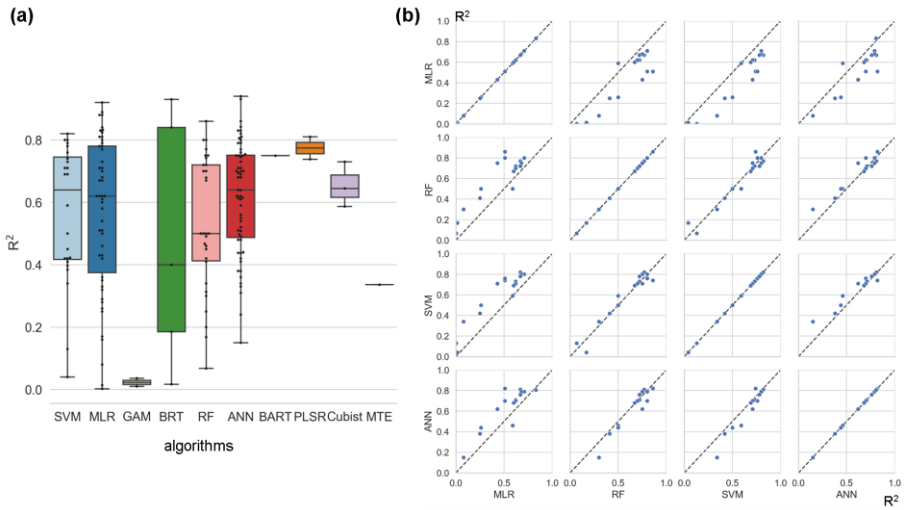

Figure 5. Differences in model accuracy (R-squared) using different algorithms across studies (a) and internal comparisons of the model accuracy (R-squared) of selected pairs of algorithms within individual studies (b). Regression algorithms: Random Forests (RF), Multiple Linear Regressions (MLR), Artificial Neural Networks (ANN), Support Vector Machines (SVM), Partial Least Squares Regression (PLSR), Generalized additive model (GAM), Boosted Regression Tree (BRT), Bayesian Additive Regression Trees (BART), Cubist, model tree ensembles (MTE). In panel (a), the horizontal line in the box indicates the medians. The top and bottom border lines of the box indicate the 75% and 25% percentiles, respectively.

3.2.2 Time scales

The impact of time scale on R-squared is considerable (Fig. 6), with models with larger time scales having lower average R-squared, especially when the time scale exceeds the monthly scale. The most frequently used scales were the daily, 8-day, and monthly scales. In studies where multiple time scales were used with other characteristics being the same, we found that models with half-hourly scales were significantly more accurate than models with daily scales (Fig. 6). However, the difference in accuracy between the day-scale and week-scale models is small. The accuracy of models with a monthly scale is the lowest.

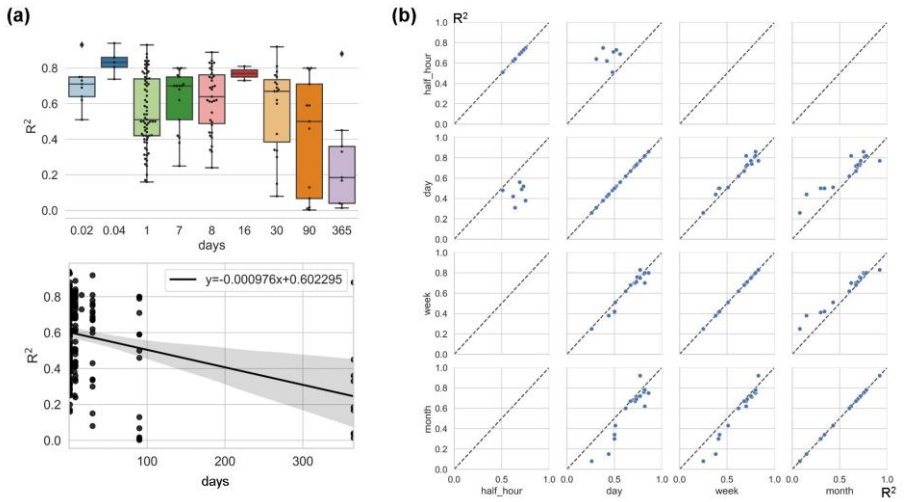

Figure 6. Differences in model accuracy (R-squared) at different time scales across studies with the linear regression between R-squared and time scales (a), and comparison of the model accuracy (R-squared) of selected pairs of time scales within individual studies (b). All model records were included in panel (a), while studies that used multiple time scales (with other model characteristics unchanged) were included in panel (b). Time scales: 0.02 days (half-hourly), 0.04 days (hourly), 30 days (monthly), and 90 days (quarterly).

3.2.3 Various predictors

Among the commonly used predictors for NEE, there are significant differences in the predictors used and their impacts on model accuracy for different PFTs (Fig. 7). Ancillary data (e.g. soil texture, soil organic content, topography) that do not have temporal variability are used less frequently because they can only explain spatial heterogeneity. In contrast, the biophysical variables LAI, FAPAR, and ET were used significantly less frequently than NDVI/EVI, especially in the cropland and wetland types. The meteorological variables Ta, Rn/Rs, and VPD were used most frequently. For forest sites, Rn/Rs and Ws appear to be the variables that improve model accuracy. For grassland sites, we found that NDVI/EVI appears to be the most effective, despite the small sample size. For sites in croplands and wetlands, we did not find predictor variables that had a significant impact on model accuracy.

For different PFTs, the top three variables in the ranking of model importance differed (Fig. S1). SM, Rn/Rs, Ta, Ts, and VPD all showed high importance across PFTs. This suggests that the variability of measured site-scale moisture and temperature conditions is important for the simulation of NEE for all PFTs. In contrast, in the importance ranking, other variables such as precipitation and NDVI/EVI may not lead because of the lag in their effect on NEE (Hao et al., 2010; Cranko Page et al., 2022). And some other variables may improve model accuracy for specific PFTs such as groundwater table depth (GWT) for wetland sites and growing degree days (GDD) for tundra sites.

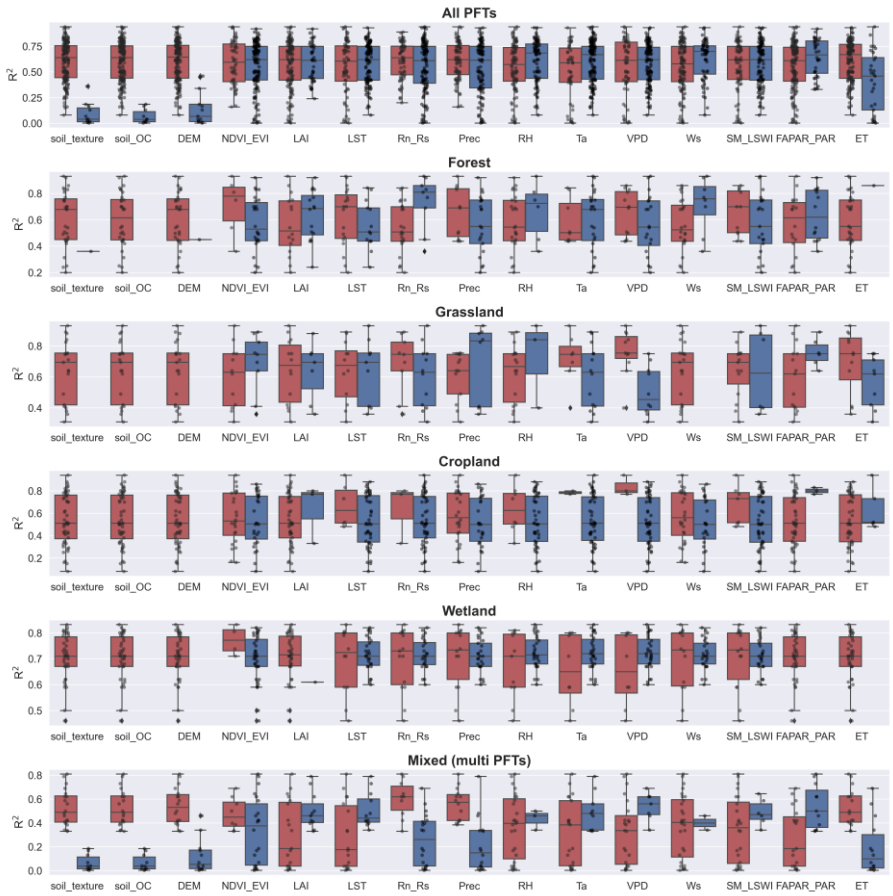

Figure 7. The impact of the various predictors incorporated in models of different PFTs (1-forest, 2-grassland, 3-cropland, 4-wetland, 6-tundra) on R-squared. Dark blue boxes indicate that the predictor was used in the model, while dark red boxes indicate that the predictor was not used. Predictors: soil organic content (Soil_OC), precipitation (Prec), soil moisture/land surface water index (SM_LSWI), net radiation/solar radiation (Rn_Rs), enhanced vegetation index (EVI), air temperature (Ta), vapor-pressure deficit (VPD), the fraction of absorbed photosynthetically active radiation/photosynthetically active radiation (FAPAR_PAR), relative humidity (RH), evapotranspiration (ET), leaf area index (LAI).

3.2.4 Other features

In addition, we evaluated other features of the model construction that may contribute to differences in model accuracy (Fig. 8). Studies at continental and global scales with a large number of sites and a large span of years correspond to lower R-squared than studies at local and regional scales, suggesting that studies with a large number of sites across large regions are likely to have high variability in the relationship between NEE and

covariates and that studies at small scales are more likely to have higher model accuracy. Spatial validation (usually 'leave one site out') corresponds to lower model accuracy compared to random and temporal validation. This again confirms the dominant role of heterogeneity in the relationship between NEE and covariates across sites in explaining model accuracy. This seems to be indirectly supported by the fact that a high ratio of training to validation sets corresponds to a low R-squared, as this high ratio tends to be accompanied by the use of the 'leave one site out' validation approach. The accuracy of the models with a growing season period was slightly higher than that of the models with an annual period. For the satellite remote sensing data used, the models based on MODIS data with biophysical variables extracted were slightly less accurate than those based on Landsat data. For the daily scale models, Landsat data performed a little better than MODIS (Fig. S2). This suggests that the higher temporal resolution of MODIS compared to Landsat may not play a dominant role in improving model accuracy. This may also be partially attributed to studies using MODIS-based explanatory data that tend to include too large surrounding areas around the site (e.g., 2x2 km), which can lead to a scale mismatch between the flux footprint and the explanatory variables.

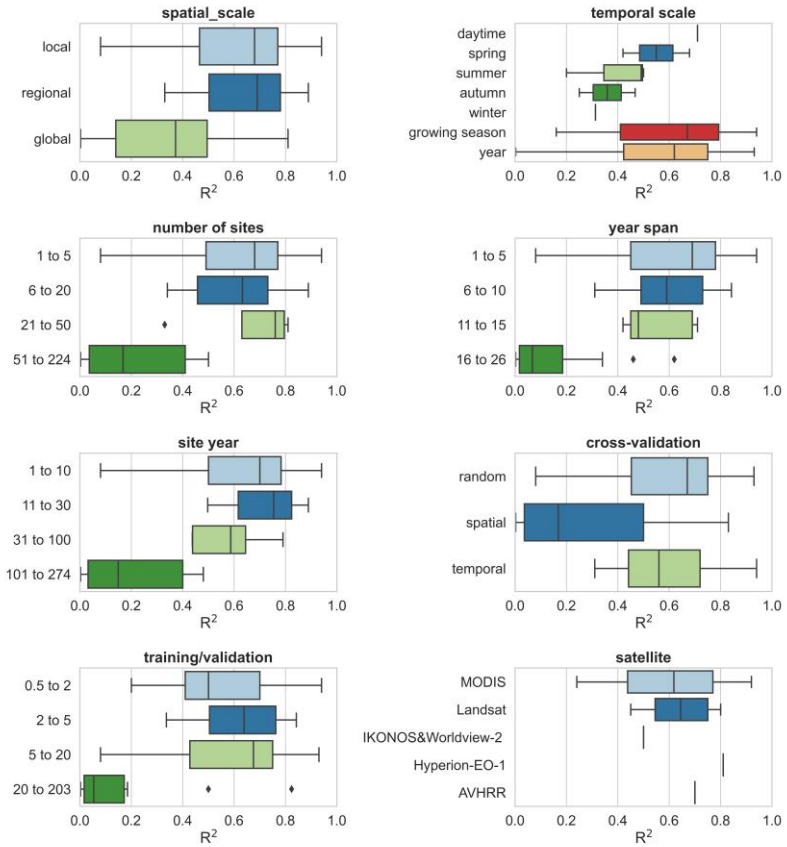

Figure 8. The impacts of other features (i.e. spatial scale, study period, number of sites, year span, site year, cross-validation method, training/validation, and satellite imagery) on the model performance.

3.3. The joint causal impacts of multi-features based on the BN

We selected the features that had a more significant impact on model accuracy in the above assessment and further incorporated them into the BN-based multivariate assessment to understand the joint impact of multiple features on R-squared. The features incorporated included the spatial scale, the number of sites, the ~~temporal~~time scale, the span of years, the cross-validation method, and whether some specific predictors were used. We discretized the distribution of individual nodes and compiled the BN (Fig. 9.a) using records from different PFTs as input. Sensitivity analysis of the R-squared node (Fig. 10) showed that R-squared was most sensitive to 'year span', cross-validation method, Rn/Rs, and time scale under multi-feature control. In the forest and cropland types, R-squared is more sensitive to Rn/Rs, while in the wetland type it is more sensitive to SM/LSWI and Ta. The sensitivity of R-squared to 'year span' was much higher in the cropland type compared to the other PFTs, which may suggest that the interannual variability in the NEE simulations of the cropland type is higher due to potential interannual variability of the planting structure and irrigation practices. For the cropland type, differences in the phenology, harvesting, and irrigation (water volume and frequency) in different years can lead to significant inter-annual differences in NEE simulations. Subsequently, using the constructed BN (with the empirical information in previous studies incorporated), for new studies we can instructively infer the probability distribution of the possible R-squared (Fig. 9.b) with some model features predetermined. In previous studies, spatio-temporal mapping of NEE based on statistical models has often lacked accuracy assessment since there are no grid-scale NEE observations, and this BN may have the potential to be used to validate the accuracy (R-squared) of the NEE time series output of the grid-scale (i.e. inferring possible R-squared from model features, where the output of the grid-scale is considered to be of the form 'leave one site out').

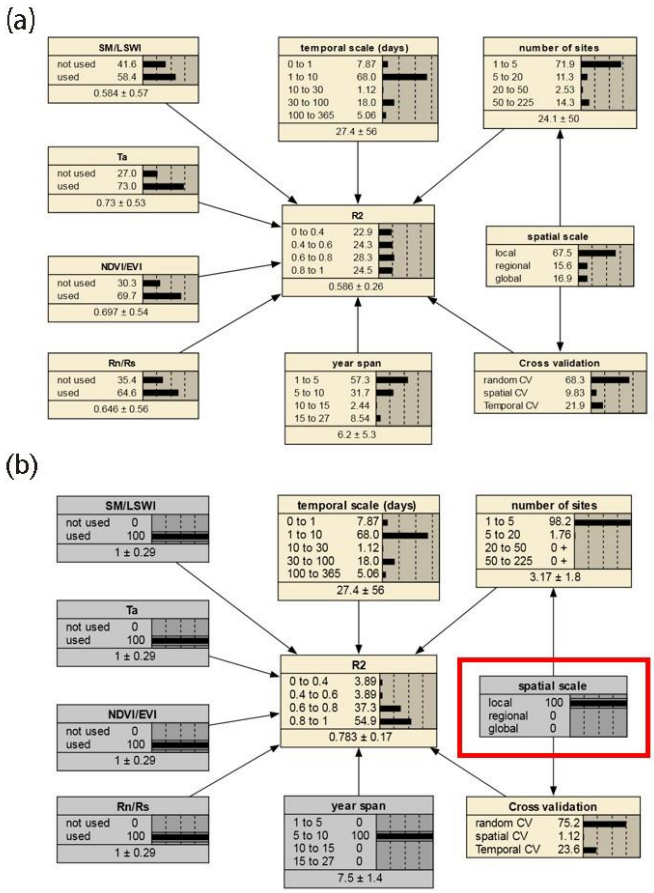

Figure 9. The joint effects of multiple features on the R-squared based on the BN with all records input (a) and the inference on the probability distribution of R-squared based on the BN with the status of some nodes determined (b). The values before and after the "±" indicate the mean and standard deviation of the distribution, respectively. The gray boxes indicate that the status of the nodes has been determined. In panel (b), specific values of parent nodes such as 'spatial scale' are determined (shown in the red box), leading to an increase in the expected R-squared compared to the average scenario of the panel (a) (as inferred from the posterior conditional probabilities with the status of the node 'spatial scale' are determined as 'local').

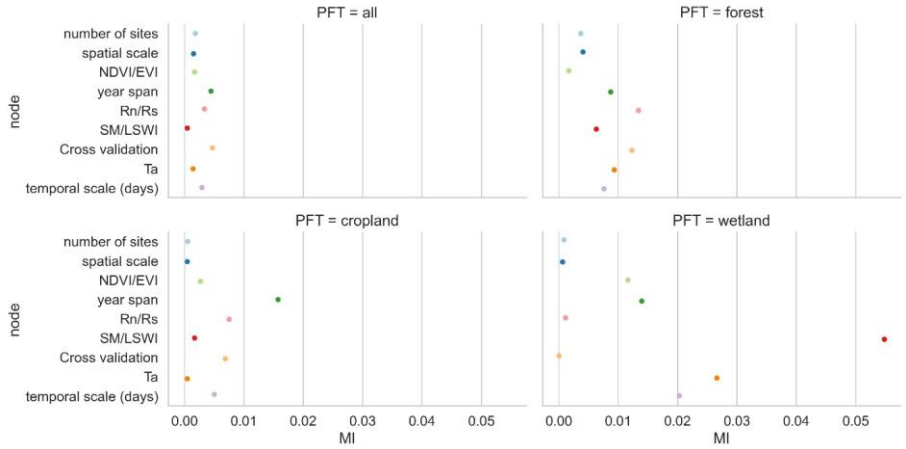

Figure 10. The sensitivity analysis of the R-squared node to other nodes based on the mutual information (MI) across PFTs. 'Cross-validation' is the cross-validation method including spatial, temporal, and random cross-validation.

4 Discussions

Many studies have evaluated the incorporation of various predictors and model features using machine learning for improving the site-scale NEE predictions ~~(Tramontana et al., 2016; Zeng et al., 2020; Jung et al., 2011)~~(Tramontana et al., 2016; Zeng et al., 2020; Jung et al., 2011). A comprehensive evaluation of these studies to provide definitive guidance on the selection of features in NEE prediction modeling is limited. This study fills the research gap with a meta-analysis of the literature through statistics on the accuracy and performance of models. Machine learning-based NEE simulations and predictions still suffer from high uncertainty. By better understanding the expected improvements that can be achieved through the inclusion of different features, we can identify priorities for the consideration of different features in modeling efforts and avoid operations decreasing model accuracy.

Compared to previous comparisons of machine learning-based NEE prediction models, this study is more comprehensive. Previous studies (Abbasian et al., 2022) have also found advantages of RF over other algorithms in NEE prediction. This study consolidated this finding using a larger amount of evidence. Previous studies (Tramontana et al., 2016) have also compared the impact of different practices in NEE prediction models based on the R-squared, such as comparing the difference in accuracy between the two predictor combinations (i.e., using only remotely sensed data and using remotely sensed data and meteorological data together). In contrast, since this study incorporated more detailed factors influencing model accuracy, the understanding of such issues was deepened. However, there are still many uncertainties and challenges in NEE prediction not clarified in this study.

4.1 Challenges in the site-scale NEE simulation and implications for other carbon flux simulations

4.1.1 Variations in time scales

In the above analysis, we found that the effect of the time scale of the model is considerable. This suggests that we should be careful in determining the time scale of the model to consider whether the predictor variables used will work at this time scale. Previous studies have reported the dependence of the NEE variability and mechanism on the time scales. On the one hand, the importance of variables affecting NEE varies at different time scales. For example, in tropical and subtropical forests in southern China (Yan et al., 2013), seasonal NEE variability is predominantly controlled by soil temperature and moisture, while interannual NEE variability is controlled by the annual precipitation variation. A study (Jung et al., 2017) showed that for annual-scale NEE variability, water availability and temperature were the dominant drivers at the local and global scales, respectively. This indicates the need to recognize the temporal and spatial driving mechanisms of NEE in advance in the development of NEE prediction models. On the other hand, dependence may exist between NEE anomalies at various time scales. For example, previous studies (Luyssaert et al., 2007) showed that short-term temperature anomalies may interpret both the daily and seasonal NEE anomalies. This implies that the models at different time scales may not be independent. In the previous studies, the relationship between prediction models at different scales has not been well investigated, and it may be valuable to compare the relations between data and models at different scales in depth. Larger time scales correspond to lower model accuracy, possibly related to the fact that some small-time-scale relations between NEE and covariates (especially meteorological variables) are smoothed. In particular, for models with time scales smaller than one day (e.g. half-hourly models), the 8-daily and 16-daily biophysical variable data obtained from satellite remote sensing are difficult to explain the temporal variation in the sub-daily NEE. Therefore, for models at small time scales (i.e. half-hourly, hourly, daily scale models), in situ meteorological variables may be more important. The inclusion of some ancillary variables (e.g. soil texture, topographic variables) with no temporal dynamic information may be ineffective unless many sites are included in the model and the spatial variability of the ancillary variables for these sites is sufficiently large (Virkkala et al., 2021).

In terms of completeness and purity of training data, hourly and daily models can be better compared to monthly and yearly models. Hourly and daily models can usually preclude those low-quality data and gaps in the flux observations. However, for monthly and yearly scale models, gap-filling (Ruppert et al., 2006; Moffat et al., 2007; Zhu et al., 2022) is necessary because there are few complete and continuous fluxes observations without data gaps on the monthly to yearly scales. Since various gap-filling techniques rely on environmental factors (Moffat et al., 2007) such as meteorological observations, this may introduce uncertainty in the predictive models (i.e., a small fraction of the observed information of NEE is estimated from a combination of independent variables). How it would affect the accuracy of prediction models at various time scales remains uncertain, although various gap-filling techniques have been widely used in the pre-processing of training data.

In addition, the impacts of lagged effects (Hao et al., 2010; Cranko Page et al., 2022) of covariates are not considered in most models, which may underestimate the degree of explanation of NEE for some predictor variables (e.g. precipitation). Most of the machine learning-based models use only the average Ta and do not take into account the maximum temperature, minimum temperature, daily difference in temperature, etc., as in

the process-based ecological models (Mitchell et al., 2009). This suggests that the inclusion of different temporal characteristics of individual variables in machine learning-based NEE prediction models may be insufficient.

4.1.2 Scale mismatch of explanatory predictors and flux footprints

An excessively large extraction area of remote sensing data (e.g., 2x2 km) may be inappropriate. In the non-homogeneous underlying conditions, the agreement of the area of flux footprints with the scale of the predictors should be considered in the extraction of the predictor variables in various PFTs (Chu et al., 2021).

The effects of this mismatch between explanatory variables and flux footprints may be diverse for different PFTs. For example, for cropland types, the NEE is monitored at a range of several hundred meters around the flux towers, but remote sensing variables such as FAPAR, NDVI, LAI, etc. can be extracted at coarse scales (e.g., 2x2 km), some effects outside the extent of the flux footprint (Chu et al., 2021; Walther et al., 2021) are incorporated (e.g., planting structures with high spatial heterogeneity, agricultural practices such as irrigation). And for more homogeneous types such as grasslands, coarse-scale meteorological data may still cause spatial mismatches, even though the differences in land cover types within the 2x2 km and 200x200 m extent around the flux stations in grasslands may not be considerable. For example, precipitation with high spatial heterogeneity can dominate the spatial variability of soil moisture and thus affect the spatial variability of grassland NEE (Wu et al., 2011; Jongen et al., 2011). ~~However, using 0.25°x0.25° reanalysis precipitation data (Zeng et al., 2020)~~However, using 0.25°x0.25° reanalysis precipitation data (Zeng et al., 2020) may make it difficult for predictive models to capture this spatial heterogeneity around the flux station.

Since few of the studies included in this meta-analysis considered the effect of variation in flux footprint, this feature was difficult to consider in this study. However, its influence should still be further investigated in future studies. With flux footprints calculated (Kljun et al., 2015) and the factors around the flux site (Walther et al., 2021) that affect the flux footprint incorporated, .it is promising to clarify this issue.

4.1.3 Possible unbalance of training and validation sets

In addition to the time scale of the models, the most significant differences in model accuracy and performance were found in the heterogeneity within the NEE dataset and the match of the training set and validation set. Often NEE simulations can achieve high accuracy in local studies, where the main factor negatively affecting model accuracy may be the interannual variability in the relationship between NEE and covariates. However, the complexity may increase when the dataset contains a large study area, many sites, PFTs, and year spans. Under this condition, the accuracy of the model in the 'leave one site out' validation may be more dependent on the correlation and match between the training and validation sets (Jung et al., 2020). When the model is applied to an outlier site (of which the NEE, covariates, and their relationship are very different compared with the remaining sites), it appears to be difficult to achieve a high prediction accuracy ~~(Jung et al., 2020).~~(Jung et al., 2020). If we further upscale the prediction model to large spatial and ~~temporal~~time scales, the uncertainties involved may be difficult to assess ~~(Zeng et al., 2020)~~(Zeng et al., 2020). We can only infer the possible model accuracy based on the similarity of the distribution of predictors in the predicted grid to that of the existing sites

in the model. In the upscaling process, reanalysis data with the coarse spatial resolution are often used as an alternative for site-scale meteorological predictors. However, most studies did not assess in detail the possible errors associated with spatial mismatches in this operation.

In summary, the site-scale NEE predictions may require more focus on the internal heterogeneity of the NEE dataset and the matching of the training set and validation set, and also require a better understanding of the influence of different scales of the same variable (e.g. site-scale precipitation and grid-scale precipitation in the reanalysis meteorological data) across modeling and upscaling steps. For the prediction of other carbon fluxes such as methane fluxes (in the same framework as the NEE predictions), the results of this study may also be partially applicable, although there may be significant differences in the use of specific predictors (Peltola et al., 2019).

4.2 Uncertainties

The uncertainties in this analysis may include:

a) Publication bias and weighting: Publication bias is not refined due to the limitations of the number of articles that can be included. Meta-analyses often measure the quality of journals and the data availability (Borenstein et al., 2011; Field and Gillett, 2010) to determine the weighting of the literature in a comprehensive assessment. However, a high proportion of the articles in this study did not make flux observations publicly available or share the NEE prediction models developed. Furthermore, meta-analysis studies in other fields typically measure the impact of papers by evidence/data volume, and the variance of the evaluated effects (Adams et al., 1997; Don et al., 2011; Liu et al., 2018). However, in this study, because no convincing method is found to quantify the weights of results from included articles, some features (e.g. the number of flux sites, the span of years) were directly assessed rather than used to determine the weights of the articles.

b) Limitations of the criteria for inclusion in the literature: in the model accuracy-based evaluation, we selected only literature that developed multiple regression models. Potentially valuable information from univariate regression models was not included. In addition, only papers in high-quality English journals were included in this study to control for possible errors due to publication bias. However, many studies that fit this theme may have been published in other languages or other journals.

c) Independence between features: There is dependence between the evaluated features (e.g. the dependency between the spatial extent and the number of sites). It may negatively affect the assessment of the impact of individual features on the accuracy of the model, although the BN-based analysis of joint effects can reduce the impact of this dependence between variables by specifying causal relationships between features. The interference of unknown dependencies between features may still not be eliminated when we focus on the effects of an individual feature on the model performance. We should pay more attention to the effect of features on model accuracy individually in future studies, and it may be valuable to keep other features as constants while changing the level of only one feature and assessing the difference. It may help us to understand the real sensitivity of model accuracy to different features in specific conditions. The sample size collected in this study (178 records in total) is not very large. This also suggests that more future efforts should be devoted to the comprehensive evaluation and summarization of NEE simulations.

Additionally, there are still other potential factors not considered by this study such as the uncertainty of climate data (site vs reanalysis), footprint matching between site and satellite images, etc. Overall, although the quantitative results of this study should be used with caution, they still have positive implications for guiding future such studies.

5 Conclusion

We performed a meta-analysis of the site-scale NEE simulations combining in situ flux observations, meteorological, biophysical, and ancillary predictors, and machine learning. The impacts of various features throughout the modeling process on the accuracy of the model were evaluated. The main findings of this study include:

1. RF and SVM performed better than other evaluated algorithms.
2. The impact of time scale on model performance is significant. Models with larger time scales have lower average R-squared, especially when the time scale exceeds the monthly scale. Models with half-hourly scales (average R-squared = 0.73) were significantly more accurate than models with daily scales (average R-squared = 0.5).
3. Among the commonly used predictors for NEE, there are significant differences in the predictors used and their impacts on model accuracy for different PFTs.
4. It is necessary to focus on the potential imbalance between the training and validation sets in NEE simulations. Studies at continental and global scales (average R-squared = 0.37) with multiple PFTs, more sites, and a large span of years correspond to lower R-squared than studies at local (average R-squared = 0.69) and regional scales (average R-squared = 0.7).

Acknowledgments

We thank the editors and three anonymous referees for their insightful comments on this paper which substantially improved.

Financial support

This research was supported by the National Natural Science Foundation of China (Grant No. U1803243), the Key projects of the Natural Science Foundation of Xinjiang Autonomous Region (Grant No. 2022D01D01), the Strategic Priority Research Program of the Chinese Academy of Sciences (Grant No. XDA20060302), and High-End Foreign Experts Project.

~~**Contributions**~~

Author contributions

H.S and G.L initiated this research and were responsible for the integrity of the work as a whole. H.S performed formal analysis, and calculations and drafted the manuscript. H.S, G.L, X.M, X.Y, Y.W, W.Z, M.X, C.Z, and Y.Z were responsible for the data collection and analysis. G.L, P.D.M, T.V.D.V, O.H, and A.K contributed resources and financial support.

Competing interests

The authors declare that they have no conflict of interest.

Data availability

The data used in this study can be accessed by contacting the first author (~~shihaiyang16@mails.ucas.ac.cn~~shihaiyang16@mails.ucas.ac.cn) based on a reasonable request.

Code availability

The code used in this study can be accessed by contacting the first author (~~shihaiyang16@mails.ucas.ac.cn~~shihaiyang16@mails.ucas.ac.cn) based on a reasonable request.

References

Abbasian, H., Solgi, E., Mohsen Hosseini, S., and Hossein Kia, S.: Modeling terrestrial net ecosystem exchange using machine learning techniques based on flux tower measurements, Ecological Modelling, 466, 109901, https://doi.org/10.1016/j.ecolmodel.2022.109901, 2022.

Adams, D. C., Gurevitch, J., and Rosenberg, M. S.: Resampling tests for meta‐analysis of ecological data, Ecology, 78, 1277–1283, 1997.

Baldocchi, D. D.: Assessing the eddy covariance technique for evaluating carbon dioxide exchange rates of ecosystems: past, present and future, 9, 479–492, https://doi.org/10.1046/j.1365-2486.2003.00629.x, 2003.

Berryman, E. M., Vanderhoof, M. K., Bradford, J. B., Hawbaker, T. J., Henne, P. D., Burns, S. P., Frank, J. M., Birdsey, R. A., and Ryan, M. G.: Estimating soil respiration in a subalpine landscape using point, terrain, climate, and greenness data, Journal of Geophysical Research: Biogeosciences, 123, 3231–3249, 2018.

Borenstein, M., Hedges, L. V., Higgins, J. P., and Rothstein, H. R.: Introduction to meta-analysis, John Wiley & Sons, 2011.

Cho, S., Kang, M., Ichii, K., Kim, J., Lim, J.-H., Chun, J.-H., Park, C.-W., Kim, H. S., Choi, S.-W., and Lee, S.-H.: Evaluation of forest carbon uptake in South Korea using the national flux tower network, remote sensing, and data-driven technology, Agricultural and Forest Meteorology, 311, 108653, 2021.

Chu, H., Luo, X., Ouyang, Z., Chan, W. S., Dengel, S., Biraud, S. C., Torn, M. S., Metzger, S., Kumar, J., Arain, M. A., Arkebauer, T. J., Baldocchi, D., Bernacchi, C., Billesbach, D., Black, T. A., Blanken, P. D., Bohrer, G., Bracho, R., Brown, S., Brunsell, N. A., Chen, J., Chen, X., Clark, K., Desai, A. R., Duman, T., Durden, D., Fares, S., Forbrich, I., Gamon, J. A., Gough, C. M., Griffis, T., Helbig, M., Hollinger, D., Humphreys, E., Ikawa, H., Iwata, H., Ju, Y., Knowles, J. F., Knox, S. H., Kobayashi, H., Kolb, T., Law, B., Lee, X., Litvak, M., Liu, H., Munger, J. W., Noormets, A., Novick, K., Oberbauer, S. F., Oechel, W., Oikawa, P., Papuga, S. A., Pendall, E., Prajapati, P., Prueger, J., Quinton, W. L., Richardson, A. D., Russell, E. S., Scott, R. L., Starr, G., Staebler, R., Stoy, P. C., Stuart-Haëntjens, E., Sonnentag, O., Sullivan, R. C., Suyker, A., Ueyama, M., Vargas, R., Wood, J. D., and Zona, D.: Representativeness of Eddy-Covariance flux footprints for areas surrounding AmeriFlux sites, Agricultural and Forest Meteorology, 301–302, 108350, https://doi.org/10.1016/j.agrformet.2021.108350, 2021.

Cleverly, J., Vote, C., Isaac, P., Ewenz, C., Harahap, M., Beringer, J., Campbell, D. I., Daly, E., Eamus, D., He, L., Hunt, J., Grace, P., Hutley, L. B., Laubach, J., McCaskill, M., Rowlings, D., Rutledge Jonker, S., Schipper, L. A., Schroder, I., Teodosio, B., Yu, Q., Ward, P. R., Walker, J. P., Webb, J. A., and Grover, S. P. P.: Carbon, water and energy fluxes in agricultural systems of Australia and New Zealand, 287, https://doi.org/10.1016/j.agrformet.2020.107934, 2020.

Cranko Page, J., De Kauwe, M. G., Abramowitz, G., Cleverly, J., Hinko-Najera, N., Hovenden, M. J., Liu, Y., Pitman, A. J., and Ogle, K.: Examining the role of environmental memory in the predictability of carbon and water fluxes across Australian ecosystems, Biogeosciences, 19, 1913–1932, 2022.

Cui, X., Goff, T., Cui, S., Menefee, D., Wu, Q., Rajan, N., Nair, S., Phillips, N., and Walker, F.: Predicting carbon and water vapor fluxes using machine learning and novel feature ranking algorithms, Science of The Total Environment, 775, 145130, 2021.

Don, A., Schumacher, J., and Freibauer, A.: Impact of tropical land-use change on soil organic carbon stocks – a meta-analysis, 17, 1658–1670, https://doi.org/10.1111/j.1365-2486.2010.02336.x, 2011.

Field, A. P. and Gillett, R.: How to do a meta‐analysis, British Journal of Mathematical and Statistical Psychology, 63, 665–694, 2010.

Fu, D., Chen, B., Zhang, H., Wang, J., Black, T. A., Amiro, B. D., Bohrer, G., Bolstad, P., Coulter, R., and Rahman, A. F.: Estimating landscape net ecosystem exchange at high spatial–temporal resolution based on Landsat data, an improved upscaling model framework, and eddy covariance flux measurements, Remote Sensing of Environment, 141, 90–104, 2014.

Fu, Z., Stoy, P. C., Poulter, B., Gerken, T., Zhang, Z., Wakbulcho, G., and Niu, S.: Maximum carbon uptake rate dominates the interannual variability of global net ecosystem exchange, Global Change Biology, 25, 3381–3394, 2019.

Hao, Y., Wang, Y., Mei, X., and Cui, X.: The response of ecosystem CO2 exchange to small precipitation pulses over a temperate steppe, Plant Ecol, 209, 335–347, https://doi.org/10.1007/s11258-010-9766-1, 2010.

Harris, N. L., Gibbs, D. A., Baccini, A., Birdsey, R. A., de Bruin, S., Farina, M., Fatoyinbo, L., Hansen, M. C., Herold, M., Houghton, R. A., Potapov, P. V., Suarez, D. R., Roman-Cuesta, R. M., Saatchi, S. S., Slay, C. M., Turubanova, S. A., and Tyukavina, A.: Global maps of twenty-first century forest carbon fluxes, Nat. Clim. Chang., 11, 234–240, https://doi.org/10.1038/s41558-020-00976-6, 2021.

Huemmrich, K. F., Campbell, P., Landis, D., and Middleton, E.: Developing a common globally applicable method for optical remote sensing of ecosystem light use efficiency, Remote Sensing of Environment, 230, 111190, 2019.

Jongen, M., Pereira, J. S., Aires, L. M. I., and Pio, C. A.: The effects of drought and timing of precipitation on the inter-annual variation in ecosystem-atmosphere exchange in a Mediterranean grassland, Agricultural and Forest Meteorology, 151, 595–606, https://doi.org/10.1016/j.agrformet.2011.01.008, 2011.

Jung, M., Reichstein, M., Margolis, H. A., Cescatti, A., Richardson, A. D., Arain, M. A., Arneth, A., Bernhofer, C., Bonal, D., and Chen, J.: Global patterns of land‐atmosphere fluxes of carbon dioxide, latent heat, and sensible heat derived from eddy covariance, satellite, and meteorological observations, Journal of Geophysical Research: Biogeosciences, 116, 2011.

Jung, M., Reichstein, M., Schwalm, C. R., Huntingford, C., Sitch, S., Ahlström, A., Arneth, A., Camps-Valls, G., Ciais, P., Friedlingstein, P., Gans, F., Ichii, K., Jain, A. K., Kato, E., Papale, D., Poulter, B., Raduly, B., Rödenbeck, C., Tramontana, G., Viovy, N., Wang, Y.-P., Weber, U., Zaehle, S., and Zeng, N.: Compensatory water effects link yearly global land CO2 sink changes to temperature, 541, 516–520, https://doi.org/10.1038/nature20780, 2017.

Jung, M., Schwalm, C., Migliavacca, M., Walther, S., Camps-Valls, G., Koirala, S., Anthoni, P., Besnard, S., Bodesheim, P., Carvalhais, N., Chevallier, F., Gans, F., S Goll, D., Haverd, V., Köhler, P., Ichii, K., K Jain, A., Liu, J., Lombardozzi, D., E M S Nabel, J., A Nelson, J., O'Sullivan, M., Pallandt, M., Papale, D., Peters, W., Pongratz, J., Rödenbeck, C., Sitch, S., Tramontana, G., Walker, A., Weber, U., and Reichstein, M.: Scaling carbon fluxes from eddy covariance sites to globe: Synthesis and evaluation of the FLUXCOM approach, 17, 1343–1365, https://doi.org/10.5194/bg-17-1343-2020, 2020.

631 Kaur, H., Pannu, H. S., and Malhi, A. K.: A Systematic Review on Imbalanced Data Challenges in
632 Machine Learning: Applications and Solutions, ACM Comput. Surv., 52, 79:1-79:36,
633 https://doi.org/10.1145/3343440, 2019.

634 Kljun, N., Calanca, P., Rotach, M., and Schmid, H. P.: A simple two-dimensional parameterisation for
635 Flux Footprint Prediction (FFP), Geoscientific Model Development, 8, 3695–3713, 2015.

636 Liu, Q., Zhang, Y., Liu, B., Amonette, J. E., Lin, Z., Liu, G., Ambus, P., and Xie, Z.: How does
637 biochar influence soil N cycle? A meta-analysis, Plant and soil, 426, 211–225, 2018.

638 Luyssaert, S., Janssens, I. A., Sulkava, M., Papale, D., Dolman, A. J., Reichstein, M., Hollmén, J.,
639 Martin, J. G., Suni, T., Vesala, T., Loustau, D., Law, B. E., and Moors, E. J.: Photosynthesis drives
640 anomalies in net carbon-exchange of pine forests at different latitudes, 13, 2110–2127,
641 https://doi.org/10.1111/j.1365-2486.2007.01432.x, 2007.

642 Marcot, B. G. and Hanea, A. M.: What is an optimal value of k in k-fold cross-validation in discrete
643 Bayesian network analysis?, Comput Stat, 36, 2009–2031, https://doi.org/10.1007/s00180-020-00999-
644 9, 2021.

645 Mitchell, S., Beven, K., and Freer, J.: Multiple sources of predictive uncertainty in modeled estimates
646 of net ecosystem CO2 exchange, Ecological Modelling, 220, 3259–3270,
647 https://doi.org/10.1016/j.ecolmodel.2009.08.021, 2009.

648 Moffat, A. M., Papale, D., Reichstein, M., Hollinger, D. Y., Richardson, A. D., Barr, A. G.,
649 Beckstein, C., Braswell, B. H., Churkina, G., Desai, A. R., Falge, E., Gove, J. H., Heimann, M., Hui,
650 D., Jarvis, A. J., Kattge, J., Noormets, A., and Stauch, V. J.: Comprehensive comparison of gap-filling
651 techniques for eddy covariance net carbon fluxes, 147, 209–232,
652 https://doi.org/10.1016/j.agrformet.2007.08.011, 2007.

653 Moffat, A. M., Beckstein, C., Churkina, G., Mund, M., and Heimann, M.: Characterization of
654 ecosystem responses to climatic controls using artificial neural networks, 16, 2737–2749,
655 https://doi.org/10.1111/j.1365-2486.2010.02171.x, 2010.

656 Moher, D., Liberati, A., Tetzlaff, J., Altman, D. G., and Prisma Group: Preferred reporting items for
657 systematic reviews and meta-analyses: the PRISMA statement, PLoS medicine, 6, e1000097, 2009.

658 Moon, T. K.: The expectation-maximization algorithm, 13, 47–60, 1996.

659 Papale, D. and Valentini, R.: A new assessment of European forests carbon exchanges by eddy fluxes
660 and artificial neural network spatialization, 9, 525–535, https://doi.org/10.1046/j.1365-
661 2486.2003.00609.x, 2003.

662 Park, S.-B., Knohl, A., Lucas-Moffat, A. M., Migliavacca, M., Gerbig, C., Vesala, T., Peltola, O.,
663 Mammarella, I., Kolle, O., Lavrič, J. V., Prokushkin, A., and Heimann, M.: Strong radiative effect
664 induced by clouds and smoke on forest net ecosystem productivity in central Siberia, Agricultural and
665 Forest Meteorology, 250–251, 376–387, https://doi.org/10.1016/j.agrformet.2017.09.009, 2018.

666 Pearl, J.: Bayesian netwcrks: A model cf self-activated memory for evidential reasoning, in:
667 Proceedings of the 7th Conference of the Cognitive Science Society, University of California, Irvine,
668 CA, USA, 15–17, 1985.

669 Peltola, O., Vesala, T., Gao, Y., Räty, O., Alekseychik, P., Aurela, M., Chojnicki, B., Desai, A. R.,
670 Dolman, A. J., Euskirchen, E. S., Friborg, T., Göckede, M., Helbig, M., Humphreys, E., Jackson, R.
671 B., Jocher, G., Joos, F., Klatt, J., Knox, S. H., Kowalska, N., Kutzbach, L., Lienert, S., Lohila, A.,
672 Mammarella, I., Nadeau, D. F., Nilsson, M. B., Oechel, W. C., Peichl, M., Pypker, T., Quinton, W.,

673 Rinne, J., Sachs, T., Samson, M., Schmid, H. P., Sonnentag, O., Wille, C., Zona, D., and Aalto, T.:
674 Monthly gridded data product of northern wetland methane emissions based on upscaling eddy
675 covariance observations, Earth System Science Data, 11, 1263–1289, https://doi.org/10.5194/essd-11-
676 1263-2019, 2019.

677 Reed, D. E., Poe, J., Abraha, M., Dahlin, K. M., and Chen, J.: Modeled Surface-Atmosphere Fluxes
678 From Paired Sites in the Upper Great Lakes Region Using Neural Networks, Journal of Geophysical
679 Research: Biogeosciences, 126, https://doi.org/10.1029/2021JG006363, 2021.

680 Reichstein, M., Camps-Valls, G., Stevens, B., Jung, M., Denzler, J., Carvalhais, N., and Prabhat:
681 Deep learning and process understanding for data-driven Earth system science, 566, 195–204,
682 https://doi.org/10.1038/s41586-019-0912-1, 2019.

683 Reitz, O., Graf, A., Schmidt, M., Ketzler, G., and Leuchner, M.: Upscaling Net Ecosystem Exchange
684 Over Heterogeneous Landscapes With Machine Learning, 126, e2020JG005814,
685 https://doi.org/10.1029/2020JG005814, 2021.

686 Ruppert, J., Mauder, M., Thomas, C., and Lüers, J.: Innovative gap-filling strategy for annual sums of
687 CO2 net ecosystem exchange, 138, 5–18, https://doi.org/10.1016/j.agrformet.2006.03.003, 2006.

688 Shi, H., Luo, G., Zheng, H., Chen, C., Bai, J., Liu, T., Ochege, F. U., and De Maeyer, P.: Coupling the
689 water-energy-food-ecology nexus into a Bayesian network for water resources analysis and
690 management in the Syr Darya River basin, Journal of Hydrology, 581, 124387,
691 https://doi.org/10.1016/j.jhydrol.2019.124387, 2020.

692 Shi, H., Hellwich, O., Luo, G., Chen, C., He, H., Ochege, F. U., Van de Voorde, T., Kurban, A., and
693 de Maeyer, P.: A global meta-analysis of soil salinity prediction integrating satellite remote sensing,
694 soil sampling, and machine learning, 1–15, https://doi.org/10.1109/TGRS.2021.3109819, 2021.

695 Tian, X., Yan, M., van der Tol, C., Li, Z., Su, Z., Chen, E., Li, X., Li, L., Wang, X., Pan, X., Gao, L.,
696 and Han, Z.: Modeling forest above-ground biomass dynamics using multi-source data and
697 incorporated models: A case study over the qilian mountains, Agricultural and Forest Meteorology,
698 246, 1–14, https://doi.org/10.1016/j.agrformet.2017.05.026, 2017.

699 Tramontana, G., Jung, M., Schwalm, C. R., Ichii, K., Camps-Valls, G., Ráduly, B., Reichstein, M.,
700 Arain, M. A., Cescatti, A., Kiely, G., Merbold, L., Serrano-Ortiz, P., Sickert, S., Wolf, S., and Papale,
701 D.: Predicting carbon dioxide and energy fluxes across global FLUXNET sites with regression
702 algorithms, Biogeosciences, 13, 4291–4313, https://doi.org/10.5194/bg-13-4291-2016, 2016.

703 Van Hulse, J., Khoshgoftaar, T. M., and Napolitano, A.: Experimental perspectives on learning from
704 imbalanced data, in: Proceedings of the 24th international conference on Machine learning, New
705 York, NY, USA, 935–942, https://doi.org/10.1145/1273496.1273614, 2007.

706 Virkkala, A.-M., Aalto, J., Rogers, B. M., Tagesson, T., Treat, C. C., Natali, S. M., Watts, J. D.,
707 Potter, S., Lehtonen, A., Mauritz, M., Schuur, E. A. G., Kochendorfer, J., Zona, D., Oechel, W.,
708 Kobayashi, H., Humphreys, E., Goeckede, M., Iwata, H., Lafleur, P. M., Euskirchen, E. S., Bokhorst,
709 S., Marushchak, M., Martikainen, P. J., Elberling, B., Voigt, C., Biasi, C., Sonnentag, O., Parmentier,
710 F.-J. W., Ueyama, M., Celis, G., St.Louis, V. L., Emmerton, C. A., Peichl, M., Chi, J., Järveoja, J.,
711 Nilsson, M. B., Oberbauer, S. F., Torn, M. S., Park, S.-J., Dolman, H., Mammarella, I., Chae, N.,
712 Poyatos, R., López-Blanco, E., Christensen, T. R., Kwon, M. J., Sachs, T., Holl, D., and Luoto, M.:
713 Statistical upscaling of ecosystem CO2 fluxes across the terrestrial tundra and boreal domain:
714 Regional patterns and uncertainties, Global Change Biology, 27, 4040–4059,
715 https://doi.org/10.1111/gcb.15659, 2021.

716 Walther, S., Besnard, S., Nelson, J. A., El-Madany, T. S., Migliavacca, M., Weber, U., Ermida, S. L.,
717 Brümmer, C., Schrader, F., Prokushkin, A. S., Panov, A. V., and Jung, M.: Technical note: A view
718 from space on global flux towers by MODIS and Landsat: The FluxnetEO dataset, Biogeosciences
719 Discussions, 1–40, https://doi.org/10.5194/bg-2021-314, 2021.

720 Wu, Z., Dijkstra, P., Koch, G. W., Peñuelas, J., and Hungate, B. A.: Responses of terrestrial
721 ecosystems to temperature and precipitation change: a meta-analysis of experimental manipulation,
722 17, 927–942, https://doi.org/10.1111/j.1365-2486.2010.02302.x, 2011.

723 Yan, J., Zhang, Y., Yu, G., Zhou, G., Zhang, L., Li, K., Tan, Z., and Sha, L.: Seasonal and inter-
724 annual variations in net ecosystem exchange of two old-growth forests in southern China, Agricultural
725 and Forest Meteorology, 182–183, 257–265, https://doi.org/10.1016/j.agrformet.2013.03.002, 2013.

726 Zeng, J., Matsunaga, T., Tan, Z.-H., Saigusa, N., Shirai, T., Tang, Y., Peng, S., and Fukuda, Y.:
727 Global terrestrial carbon fluxes of 1999–2019 estimated by upscaling eddy covariance data with a
728 random forest, 7, https://doi.org/10.1038/s41597-020-00653-5, 2020.

729 Zhang, C., Brodylo, D., Sirianni, M. J., Li, T., Comas, X., Douglas, T. A., and Starr, G.: Mapping
730 CO2 fluxes of cypress swamp and marshes in the Greater Everglades using eddy covariance
731 measurements and Landsat data, Remote Sensing of Environment, 262,
732 https://doi.org/10.1016/j.rse.2021.112523, 2021.

733 Zhou, Y., Li, X., Gao, Y., He, M., Wang, M., Wang, Y., Zhao, L., and Li, Y.: Carbon fluxes response
734 of an artificial sand-binding vegetation system to rainfall variation during the growing season in the
735 Tengger Desert, Journal of Environmental Management, 266,
736 https://doi.org/10.1016/j.jenvman.2020.110556, 2020.

737 Zhu, S., Clement, R., McCalmont, J., Davies, C. A., and Hill, T.: Stable gap-filling for longer eddy
738 covariance data gaps: A globally validated machine-learning approach for carbon dioxide, water, and
739 energy fluxes, Agricultural and Forest Meteorology, 314, 108777,
740 https://doi.org/10.1016/j.agrformet.2021.108777, 2022.

741